



## PRODUCTION OF NEUTRONS FROM INTERACTIONS OF GCR-LIKE PARTICLES

L. Heilbronn, K. Frankel, K. Holabird, C. Zeitlin, M.A. McMahan, W. Rathbun, M. Cronqvist, W. Gong, Lawrence Berkeley Laboratory, Berkeley, CA 94720

R. Madey, M. Htun, M. Elaasar, B.D. Anderson, A.R. Baldwin, J. Jiang, D. Keane, A. Scott, Y. Shao, J.W. Watson, W. M. Zhang, Kent State University, Kent, OH

A. Galonsky, R. Ronningen, P. Zecher, J. Kruse, J. Wang, G.D. Westfall, S. Yenello, Michigan State University, E. Lansing, MI.

F. Deak, A. Horvath, A. Kiss, Eötvös University, Budapest, Hungary

Z. Seres, KFKI, Budapest, Hungary,

H. Schelin, CEFET, Curitiba, Brazil

C. Stronach, R. Cary, Virginia State University, Richmond, VA

### ABSTRACT

In order to help assess the risk to astronauts due to the long-term exposure to the natural radiation environment in space, an understanding of how the primary radiation field is changed when passing through shielding and tissue materials must be obtained. One important aspect of the change in the primary radiation field after passing through shielding materials is the production of secondary particles from the breakup of the primary. Neutrons are an important component of the secondary particle field due to their relatively high biological weighting factors, and due to their relative abundance, especially behind thick shielding scenarios. Because of the complexity of the problem, the estimation of the risk from exposure to the secondary neutron field must be handled using calculational techniques. However,

those calculations will need an extensive set of neutron cross section and thick-target neutron yield data in order to make an accurate assessment of the risk. In this paper we briefly survey the existing neutron-production data sets that are applicable to the space radiation transport problem, and we point out how neutron production from protons is different than neutron production from heavy ions. We also make comparisons of one the heavy-ion data sets with Boltzmann-Uehling-Uhlenbeck (BUU) calculations.

©1998 Published by Elsevier Science Ltd. All rights reserved

## 1.0 INTRODUCTION

In order to accurately determine the radiation risk to astronauts from GCR, the nature of the secondary radiation field created by the fragmentation of GCR in shielding and tissue must be understood. Due to their high penetrabilities, neutrons are an important component of the secondary radiation field, especially for astronauts protected by thick shielding on lunar or Martian bases[1]. The predominant source of neutrons is interactions of GCR in shielding materials. These interactions span the full range of GCR ions (protons, helium, and HZE) and GCR energies (100 MeV/nucleon and up), and as such neutrons are produced from an enormous set of interactions. Some studies have been conducted at ground-based accelerator facilities in regards to the production of neutrons from GCR-like interactions, but because accelerator resources are limited and because neutron experiments require a large amount of the time available at those accelerators, the best approach to the problem of determining the amount of neutron radiation behind shielding is through a calculational approach, such as the ones reported in references [1] and [2]. The models used to calculate neutron production behind thick shields will need cross-section data as input and thick-target production data for

verification of the models' output. From the viewpoint of the experimentalist, the key questions are (1) What are the important sets of data needed by theorists for the development and verification of their codes, and (2) What data sets already exist that are applicable to the problem? The answers to those questions will help in the development of an experimental program that best addresses the problems concerning the production on neutrons behind shielding in various deep-space mission scenarios.

In answer to question (1), the data will need to shed information on some of the properties of the neutron flux such as total neutron production, angular distributions, and energy distributions. In addition, details on the systematics of neutron production on projectile mass and energy and target mass will be needed. The projectiles include protons, helium, and heavy ions with atomic number as large as 26 (iron). The projectile energies should at least span the range of energies around the peak of the flux distributions, namely 100 MeV/nucleon to 2 GeV/nucleon. Target masses should include possible shielding materials such as aluminum, water, and regolith components, as well as tissue components such as water, carbon, and nitrogen.

In the following, we describe some of the experimental results which are pertinent to question (2). In addition to briefly describing those results and how they apply to the issues raised above, we also outline some of the missing gaps in the data base which we feel need to be filled.

## 2.0 NEUTRON PRODUCTION DATA SETS

Since protons make up close to 90% of the GCR flux, data in regards to the production of neutrons from proton interactions is needed. One research program has produced an extensive set of measurements of neutron production from proton

interactions in a variety of targets, including both thick-target (stopping and near-stopping target) yields and thin-target cross sections [3-6]. This set of data covers much of the data needed to describe neutron production from GCR-like protons, although additional data (such as measurements at 0 degrees) are needed.

Although helium makes up about 10% of the GCR flux and HZE makes up about 1% of the GCR flux, one calculation<sup>2</sup> predicts that about 15% of the neutron flux behind 50 g/cm<sup>2</sup> of water comes from helium interactions, and another 16% comes from HZE interactions. However, unlike the case with protons, the heavy-ion neutron data base has a scant amount of applicable data. To our knowledge, there is only one reference on neutron production from heavy-ion GCR-like particles stopping in shielding materials (177.5 MeV/nucleon and 160 MeV/nucleon helium particles stopping in C, Pb, steel, and water)[7]. There are a few references in regards to thin-target neutron cross-section data (see, for example, references [8 - 14]) that are relevant to GCR-like interactions. More data is needed in order to determine the systematics of neutron production on heavy-ion projectile mass and energy and on target mass. In order to fill in some of the missing gaps in the heavy-ion neutron data base, we have conducted two sets of accelerator-based experiments that have measured neutron yields from heavy-ion interactions.

One of those experiments was carried out at the Bevalac facility at Lawrence Berkeley Laboratory, using a 435 MeV/nucleon Nb beam stopping in a Nb target 1 cm thick (8.57 g/cm<sup>2</sup>), and using a 272 MeV/nucleon beam that was stopped in targets of 1.27-cm thick Al (3.42 g/cm<sup>2</sup>) and 0.51-cm thick Nb (4.37 g/cm<sup>2</sup>). Data was taken from 14 detectors placed between 3° and 80° in the laboratory. Neutrons were detected at energies starting from 20 MeV up to twice the beam energy per nucleon.

Figure 1 shows neutron energy spectra at  $3^\circ$ ,  $9^\circ$ ,  $16^\circ$ ,  $28^\circ$ ,  $48^\circ$ , and  $80^\circ$  for the 435 MeV/nucleon Nb + Nb system. The error bars represent statistical uncertainties only. The solid lines are BUU (Boltzmann-Uehling-Uhlenbeck) model calculations of the data.

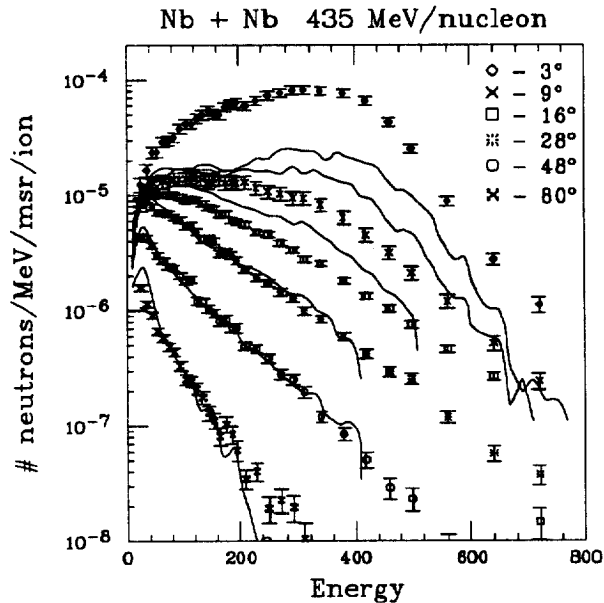


Fig 1. Thick-target neutron spectra from the 435 MeV/nucleon Nb + Nb system at the indicated angles. The solid lines come from a fit to the data using BUU calculations.

The broad peak in Figure 1 at  $3^\circ$  between 200 MeV and 400 MeV indicates a strong contribution from projectile breakup due to peripheral collisions with the target nuclei. Since the projectile may have any energy between 435 MeV/nucleon and 0 MeV at the time of collision, projectile breakup occurs over a wide range of velocities, hence the broadness of the peak at  $3^\circ$ . The spectra at  $16^\circ$ ,  $28^\circ$ ,  $48^\circ$ , and  $80^\circ$  have an exponential behavior which is typical of evaporation of fragments and nucleons from a hot source created in the overlap region between the target and projectile. There may also be some contribution from target evaporation in these

spectra, but the low energy cutoff (about 20 MeV) is too high to see most of the neutrons that come from such a source. At  $9^\circ$  there is a transition from neutron spectra dominated by projectile-like neutrons to spectra that are dominated by neutrons emitted from the decay of the overlap region. Note that neutrons with energies above the beam energy per nucleon are observed, even out to  $48^\circ$ . This is typical of the collective nature of heavy-ion collisions, where individual nucleons in the projectile and target may get a momentum boost at the time of collision due to the Fermi motion of nucleons inside a nucleus.

In general BUU calculations (solid lines in Fig. 1) do a good job of fitting the data at large angles, both in magnitude and shape. However, at the forward angles the BUU calculations either over predict or under predict the yield, depending on the angle. Even though the BUU calculation misses the magnitude of the forward angle spectra, it does a fairly good job in reproducing the shape of those spectra. Because of the method used to compare data to calculation, it is not known whether the discrepancy between the two is due to (1) the BUU-generated cross sections used as input into the calculation, or (2) the part of the calculation that generates neutrons once the input cross sections are in place. In any case, it will be necessary to measure cross section data for Nb + Nb at a variety of Nb energies in order to verify that the input into the transport calculation is valid.

It is interesting to compare the neutron yields between the 256 MeV p + Al system and the 272 MeV/nucleon Nb + Al system. Figure 2 shows the yields from both systems at  $7.5^\circ$ ,  $30^\circ$ , and  $60^\circ$  as a function of the atomic number of the projectile. At both  $30^\circ$  and  $60^\circ$  the yield from the Nb + Al system is about 10 times the yield from the p + Al system, whereas at  $7.5^\circ$  the yields differ by a factor of about 1000. This, along with the fact that there is an appreciable yield of neutrons above the beam energy per nucleon in HZE interactions, but no such yield in proton

interactions, best illustrates why the production of neutrons from HZE will need to be handled differently than in the case of production from proton interactions. The results shown here show that the production of neutrons from HZE interactions cannot be estimated reliably by a simple scaling of the neutron production from proton interactions.

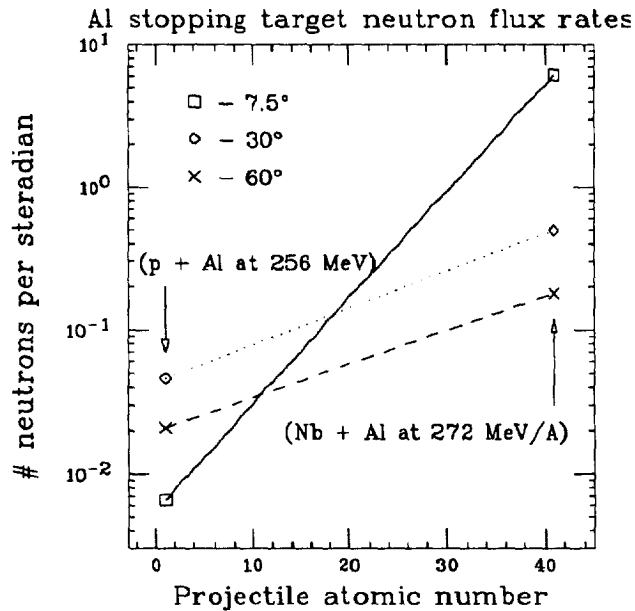


Fig. 2. Comparison of neutron yields from 256 MeV p + Al and 272 MeV/nucleon Nb + Al interactions.

Thick target neutron yields from 155 MeV/nucleon He + Al and from 155 MeV/nucleon C + Al were measured at the National Superconducting Cyclotron Laboratory at Michigan State University. In addition to the thick target yields, cross section measurements were made for C + Al at 155 MeV/nucleon and 75 MeV/nucleon. Arrays of neutron detectors were placed from 4° to 160° in the laboratory. Analysis of the data is ongoing at this time. However, some preliminary thick-target spectra can be shown. Figure 3 shows unnormalized neutron spectra at 10°, 30°, 60°, 90°, 125°, and 160° for the 155 MeV/nucleon C + Al system.

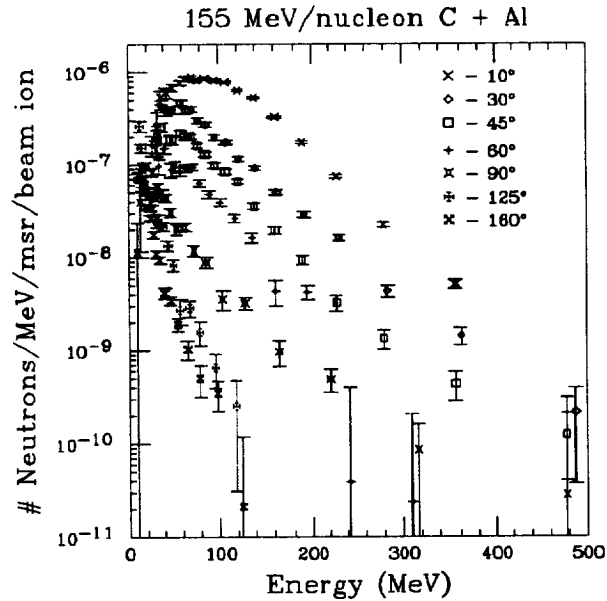


Fig. 3. Stopping-target neutron yields from 155 MeV/nucleon C + Al interactions at the indicated angles.

As with the Nb systems, there is a strong contribution from projectile-like fragmentation in the forward direction, with neutron energies as high as twice the beam energy per nucleon. The spectra at the larger angles display the typical exponential behavior of the de-excitation of the overlap region of the beam-target collision. The data from these systems will be used to provide more information on the contribution to the yield from target evaporation.

### 3.0 CONCLUSIONS

The problem of determining the flux of neutrons produced by GCR interactions in shielding must ultimately be done using calculational techniques, which in turn require experimental data for verification of both the input and output of their calculations. To date the most complete data set available is with proton-induced interactions, although there are gaps in that data set which should



be filled, such as extending the existing measurements to  $0^\circ$  and to higher incident proton energies. The set of data in regards to neutron production from heavy-ion induced interactions still requires a great deal of data in order to determine the systematics of neutron production on projectile mass and energy, target mass, production angle, and neutron energy. These systematics should cover a span of projectile energies from 100 MeV/nucleon up to 2 GeV/nucleon and projectile mass from He up to Fe. The heavy ion stopping-target data that is available (Nb + Nb and Al reactions at 435 and 272 MeV/nucleon, 177.5 MeV/nucleon He + C, Al, Pb, and water, and He and C interactions in Al at 155 MeV/nucleon) indicates that a simple scaling of proton-induced neutron yields will not reproduce the heavy-ion induced neutron yields. In addition, the comparison of the Nb + Nb with BUU calculations points to the importance of cross-section data for use in model calculations. As is the case with stopping-target data, there is an inadequate amount of cross-section data available at this time.

#### ACKNOWLEDGMENTS

The data in Figs. 1-3 were taken at the LBL Bevalac and the MSU NSCL with support from the National Aeronautics and Space Administration NASA Grant L14230C, the U.S. Department of Energy Grants Nos. DE-FG89ER40531 and DE-AC03-76SF00098, and the National Science Foundation Grants Nos. PHY-91-07064, PHY-88-02392, and PHY-86-11210. The work of the LBNL group is supported by the NASA Space Radiation Health Program.

#### REFERENCES

1. L. C. Simonsen and J.E. Nealy, Radiation Protection for Human Missions to the Moon and Mars, *NASA Technical Paper 3079*, 1991

2. F.A. Cucinotta, Calculations of Cosmic-Ray Helium Transport in Shielding Materials, *NASA Technical Paper 3354*, 1993
3. M.M. Meier, D.A. Clark, C.A. Goulding, J.B. McClelland, G.L. Morgan, C.E. Moss, and W.B. Amian, Differential Neutron Production Cross Sections and Neutron Yields from Stopping-Length Targets for 113-MeV Protons, *Nucl. Sci. and Eng.* **102**, 310-321 (1989)
4. M.M. Meier, C.A. Goulding, G.L. Morgan, and J.L. Ullmann, Neutron Yields from Stopping-Length and Near-Stopping-Length Targets for 256-MeV Protons, *Nucl. Sci. and Eng.* **104**, 339-363 (1990)
5. M.M. Meier, W.B. Amian, C.A. Goulding, G.L. Morgan, and C.E. Moss, Differential Neutron Production Cross Sections for 256 MeV Protons, *Nucl. Sci. and Eng.* **110**, 289-298 (1992)
6. W.B. Amian, R.C. Byrd, D.A. Clark, C.A. Goulding, M.M. Meier, G.L. Morgan, and C.E. Moss, and Differential Neutron Production Cross Sections for 597 MeV Protons, *Nucl. Sci. and Eng.* **115**, 1-12 (1993)
7. R.A. Cecil, B.D. Anderson, A.R. Baldwin, R. Madey, A. Galonsky, P. Miller, L. Young, and F.M. Waterman, Neutron angular and energy distributions from 710-MeV alphas stopping in water, carbon, steel, and lead, and 640-MeV alphas stopping in lead, *Phys. Rev. C* **21**, 2471-2484 (1980)
8. W. Schimmerling, J.W. Kast, D. Ortendahl, R. Madey, R.A. Cecil, B.D. Anderson, and A.R. Baldwin, measurement of the Inclusive Neutron production by Relativistic Neon Ions on Uranium, *Phys. Rev. Lett.* **43**, 1985-1987 (1979)

9. R.A. Cecil, B.D. Anderson, A.R. Baldwin, R. Madey, W. Schimmerling, J.W. Kast, and D. Ortendahl, Inclusive neutron production by 337 MeV/nucleon neon ions on carbon, aluminum, copper, and uranium, *Phys. Rev. C* **24**, 2013-2029 (1981)
10. R. Madey, B.D. Anderson, R.A. Cecil, and P.C. Tandy, Total inclusive neutron cross sections and multiplicities in nucleus-nucleus collisions at intermediate energies, *Phys. Rev. C* **28**, 706-709 (1983)
11. R. Madey, J. Varga, A.R. Baldwin, B.D. Anderson, R.A. Cecil, G. Fai, P.C. Tandy, J.W. Watson, and G.D. Westfall, Inclusive Neutron Spectra at  $0^\circ$  from the Reactions  $Pb(Ne,n)X$  and  $NaF(Ne,n)X$  at 390 and 790 MeV per Nucleon, *Phys. Rev. Lett.* **55**, 1453-1456 (1985)
12. R. Madey, W.-M. Zhang, B.D. Anderson, A.R. Baldwin, M. Elaasar, B.S. Flanders, D. Keane, W. Pairsuwan, J. Varga, J.W. Watson, G.D. Westfall, C. Hartnack, H. Stöcker, and K. Frankel, Inclusive neutron cross sections at forward angles from Nb-Nb and Au-Au collisions at 800 MeV/nucleon, *Phys. Rev. C* **46**, 1068-1076 (1990)
13. A.R. Baldwin, R. Madey, W.-M. Zhang, B.D. Anderson, D. Keane, J. Varga, J.W. Watson, G.D. Westfall, K. Frankel, and C. Gale, Inclusive neutron cross sections from Ne-Pb collisions at 790 MeV/nucleon, *Phys. Rev. C* **46**, 258-264 (1992)
14. H.R. Schelin, A. Galonsky, C.K. Gelbke, H. Hama, L. Heilbronn, D. Krofcheck, W.G. Lynch, D. Sackett, M.B. Tsang, X. Yang, F. Deak, A. Horvath, A. Kiss, Z. Seres, J. Kasagi and T. Murakami, Neutron Production in Heavy-Ion Reactions at 35 and 50 MeV/Nucleon, *Nucl. Sci. and Eng.* **113**, 184-188, (1993)